

Hyperspectral image classification with spectral-spatial feature integration and ensemble learning

Bhavatarini Nagendra^{1,2}, Jyothi Aracot Prashant¹

¹Department of Computer Science and Engineering, M. S. Ramaiah University of Applied Sciences, Bengaluru, India

²Department of Computer Science and Engineering, REVA University, Bengaluru, India

Article Info

Article history:

Received Sep 23, 2023

Revised Oct 22, 2023

Accepted Dec 3, 2023

Keywords:

Classification

Ensemble learning

Hyperspectral image

Machine learning

Spectral-spatial feature

ABSTRACT

Hyperspectral imaging (HSI) has emerged as a robust remote sensing and medical imaging tool. However, HSI classification remains a challenging problem due to the high-dimensional data and the need for efficient feature selection and enhancement techniques. The proposed work addresses the problem of spatial feature extraction in spectral-spatial HSI classification tasks. This paper introduces an innovative model addressing the intricacies of spatial feature extraction in spectral-spatial HSI classification tasks, employing a fusion of spectral and spatial features through an adaptive kernel-based Gaussian filtering mechanism to elevate the quality of HSI data and augment classification performance. The classification is executed using three distinct classifiers, whose decisions are harmoniously integrated within an ensemble learning framework to optimize outcomes. The effectiveness of the proposed system is meticulously evaluated across three diverse datasets, Indian Pine, Pavia, and Salinas. This study also compares the model's efficiency against the existing similar work presented in the literature. The results show that the proposed work outperforms existing methods with constantly showing 99% accuracy and kappa score for each dataset, demonstrating its potential applications in various domains such as remote sensing and medical imaging.

This is an open access article under the [CC BY-SA](#) license.



Corresponding Author:

Bhavatarini Nagendra

Department of Computer Science and Engineering, REVA University

Bengaluru, Karnataka, India

Email: bhavatarini.n@reva.edu.in

1. INTRODUCTION

Hyperspectral imaging (HSI) is a powerful tool for remote sensing and image analysis, allowing for capturing spectral information across a range of electromagnetic wavelengths [1]. HSI has numerous applications in agriculture, mineral exploration, environmental monitoring, and military surveillance. However, the high-dimensional nature of HSI data, noise, and other artifacts pose significant challenges for processing and analysis [2]. In recent years, there has been a growing interest in developing advanced HSI processing and analysis techniques, such as sophisticated feature engineering mechanism, and machine learning and deep learning-based classification models [3]. Feature selection techniques are used to reduce the dimensionality of HSI data by identifying the most relevant spectral bands for classification [4]. Machine learning and deep learning methods such as k-nearest neighbors (KNN) [5], support vector machines (SVM) and convolutional neural network (CNN) [6], has been widely used to classify HSI data into different land cover types. However, due to inherent issues associated with HSI data [7], [8], building a simple and computationally efficient method with affecting the classification accuracy is a challenging task [9], [10]. One of the main research gaps in this area is developing methods that can handle the high dimensionality of

HSI data while still maintaining high classification accuracy [11]. Another significant challenge is developing a method that can effectively handle the spectral and spatial variability in HSI data and the limited training data and class imbalance issues [12]. Additionally, there is a need for methods that can handle the heterogeneous nature of HSI data, where different data sets may exhibit different characteristics and require different processing approaches [13].

This paper proposes a unique and lightweight HSI classification model combining principal component analysis (PCA)-based spectral feature selection, and adaptive Gaussian-based spatial feature enhancement. The proposed study also shows effectiveness of using an application of ensemble learning based classification task. The proposed model aims to improve the accuracy and reliability of HSI classification by addressing the pixel mixing problem by enhancing the spectral and spatial features of the data. Although, in the recent years, many researchers have focused on leveraging advantage of both spectral feature and spatial feature [14]. Spectral feature selection involves selecting the most informative spectral bands from the original HSI data to reduce the dimensionality of the data and remove irrelevant or redundant information. On the other hand, spatial feature enhancement aims to enhance the spatial features of the HSI data by selectively smoothing the data while preserving important edge and detail information. Cen *et al.* [15] showed potential of using as PCA for feature extraction, Nakamura *et al.* [16] adopted independent component analysis, and an application of non-negative matrix factorization has been adopted in [17], [18] to extract relevant features from the hyperspectral data. Demarchi *et al.* [19] presented recursive feature elimination technique for feature selection techniques, and mutual information-based feature selection, have also been explored by the study of Feng *et al.* [20] to select the most informative features for classification. However, domain adaptation is an important consideration in HSI classification, as the HSI data may come from a different domain than the training data. Researchers have also explored domain adaptation techniques, such as transfer learning [21] and domain adaptation via adversarial training [22], to address overfitting and disaster dimensionality problem associated with deep learning classification task. Based on the literature analysis it has been analyze that PCA based approaches has been widely used as a preprocessing technique and spectral feature technique. In addition to classical feature extraction, several researchers have also shown potential of using supervised machine learning classifiers for feature extraction and HIS data classification. Among many supervised classifiers in the context of HSI classification, KNN has been widely adopted due to its simplicity, high accuracy, and ability to handle non-linear data. However, KNN is often called as lazy learner as it is computationally expensive for large dataset like HSI and dependent on the choice of parameters, such as the number of neighbors, distance metric, and weighting scheme as reported in Sakthivel *et al.* [23] which offers a deep understating on the application of KNN. Pathak *et al.* [24] have used SVM for both spectral-spatial feature extraction and classification. This study has shown extensive discussion on the SVM and role of utilizing spectral and spatial feature for HSI classification.

Hence it can be seen that in literature variety of methods have been presented with their own advantages and limitations. Despite significant progress made in the HSI analysis field, several challenges still need to be addressed. These challenges include high dimensionality, spectral variability, limited training data, class imbalance, and spatial variability. This problem introduces one of the significant challenges known as the pixel mixing issue, which arises when a single pixel in an image is a linear combination of the spectral signatures of multiple materials present within the pixel. This can occur due to the spatial resolution of the sensor being lower than the size of the objects being imaged or due to the overlap of spectral signatures of different materials (endmembers). The pixel mixing problem can significantly affect the accuracy of HSI classification and needs to be addressed to achieve reliable results. Therefore, despite these challenges, the research problem in HSI classification is to develop accurate and efficient algorithms that can accurately classify HSI data into different land cover types.

The problem description: HSI can be mathematically described as a three-dimensional data cube $X(i, j, \lambda)$ where the first two dimensions represent the spatial coordinates of each pixel i and j and the third dimension represents the spectral reflectance λ values for each pixel. The value of X at a specific location (i, j) and wavelength λ is given in (1):

$$X(i, j, \lambda) = X_{i,j}(\lambda) \quad (1)$$

where $X_{i,j}(\lambda)$ represents the spectral reflectance value at pixel (i, j) and wavelength λ . Each pixel in the HSI data cube can be represented as a vector in L -dimensional space, where L is the number of spectral bands in the data. The vector for pixel (i, j) can be represented as (2):

$$v_{ij} = [X(i, j, 1), X(i, j, 2), X(i, j, 3), \dots, X(i, j, L)] \quad (2)$$

HSI classification involves assigning each pixel in the HSI data cube to a specific land cover type based on its spectral reflectance values. However, pixel mixing is a common phenomenon in HSI, where the spectral signature of a single pixel is a combination of the spectral signatures of multiple materials or substances within the pixel. This can occur due to the spatial resolution of the sensor being lower than the size of the objects being imaged or due to the overlap of spectral signatures of different materials (endmember). In other words, pixel mixing occurs when a single pixel in an image is a linear combination of the spectral signatures of multiple materials present within the pixel. Mathematically, a mixed pixel can be described as in (3):

$$X(i, j) = \sum_{k=1}^K \alpha(k) \times S(k)(i, j) + \varepsilon(i, j) \quad (3)$$

where $X(i, j)$ is the mixed pixel at location (i, j) in the image, K is the number of materials present within the pixel, $\alpha(k)$ is the abundance fraction of the k th material, $S(k)(i, j)$ is the spectral signature of the k th material at location (i, j) , and $\varepsilon(i, j)$ represents the noise and error present in the pixel. The solution to the pixel mixing problem can be described as (4):

$$\min \|X - SA\|_F^2, \text{subject to } 0 \leq a_{ij} \leq 1 \forall i, j \quad (4)$$

Where $\|\cdot\|_F$ denotes the Frobenius norm, S is a matrix of size $(L \times K)$ containing the spectral signatures of the K endmembers, and a_{ij} is the (i, j) -th element of matrix A of size $(K \times MN)$, where each column (α) of A represents the abundance fractions of the K endmembers such that $\alpha(k)$ in a particular pixel v_{ij} . The goal of pixel unmixing is to estimate A given X and K . The problem described in (4) is often addressed by researchers using conventional linear model which aims to determine a matrix A that minimizes the difference between the observed HSI data X and the product of the endmember spectral signatures S and the abundance fractions A . The linear model-based approach such as least squares regression involves certain assumption, which often struggle to deconvolve these mixed pixels accurately. However, this model also considers some constraints such that $0 \leq a_{ij} \leq 1$ to ensure that the abundance fractions are non-negative and sum to one for each pixel. For this, the latter studies in literature focuses on using different methods such as non-negative least squares, or convex optimization techniques. However, these approach not always hold potential solution as in many cases, real-world hyperspectral data exhibit non-linear behavior. The traditional methods for pixel unmixing, such as least squares regression, non-negative least squares, or convex optimization techniques, require solving a system of linear equations, which can be computationally expensive and may suffer from numerical instability in ill-conditioned systems. Additionally, these methods assume a linear relationship between the spectral signatures of the endmembers and the mixed pixel spectra, which may not always hold in practice.

The proposed solution: this study introduces a data driven methodology which focuses on improving the quality of training feature leveraging optimal spectral-spatial features and potential of ensemble learning mechanism to achieve higher classification accuracy. The core objective of this work is to develop an efficient yet robust model that can offer high quality classification map of HSI cube without involving hand-crafted feature engineering operations and complex learning model like CNN which is implemented in large scale by the researchers in the literature. The study intends to utilize the effectiveness of the ensemble learning methods following classical supervised classifiers, neural network model and adequate preprocessing operations. The schematic architecture of the proposed system following block-based work flow is shown in Figure 1.

The proposed system considers HSI that may contain mixed-pixel or pure-pixel information. To address this, our study initiates basic preprocessing operations on the input hyperspectral data. These operations aim to eliminate any ambiguities, ensuring precise feature extraction and enhancement. In the subsequent phase, we employ domain-based feature extraction methods for both spectral and spatial data. In HSI, spatial and spectral domains represent discrete features. Spatial features encompass structural, textural, edge, and contextual information, while spectral features derive from the irradiance of the object's surface, capturing properties associated with object materials. The proposed feature modeling approach utilizes PCA and adaptive Gaussian filtering technique to enhance spectral and spatial features, respectively. This not only reduces feature vector dimensionality but also improves separation between hyperspectral objects, providing more accurate pixel information for different classes. This is particularly beneficial for handling inter-class similarity and intra-class variability.

Therefore, our study believes that classifier performance can be enhanced by removing irrelevant features and achieving class distributions closer to the original. Following feature modeling, the proposed system generates a spectral-spatial feature vector, which is then split into training and testing datasets. The final module of the proposed system focuses on implementing both iterative and non-iterative learning model

for the HSI object classification and get classification map. The study in this phase also explores the effectiveness of the ensemble learning to achieve a enhance the generalization capacity of the different models. The rationale behind adopting ensemble modelling is that different models may struggle with specific classes or scenarios due to the complex nature of hyperspectral data. By employing ensemble learning, the study effectively addresses the variability in model performance, ensuring that the collective intelligence of all models is utilized to make classification decisions. Ensemble learning facilitates a more equitable contribution from each model, resulting in a comprehensive classification solution that accounts for varying strengths. The next section elaborates on the implementation of the proposed system for effective HSI classification task.

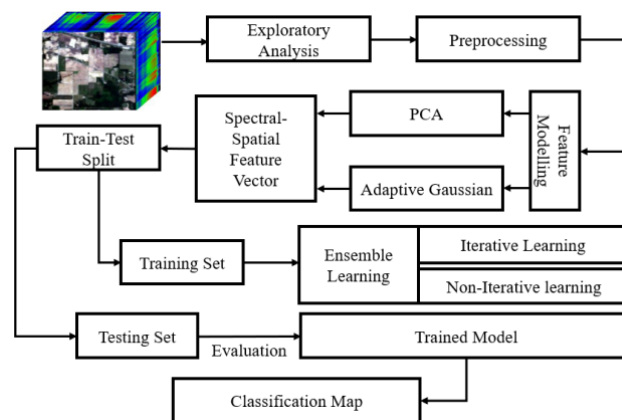


Figure 1. Block-based architecture of the proposed system for HSI classification

2. METHOD

This research methodology adopted in this study for HSI classification comprises several computational operations, including preprocessing, domain-based feature extraction and classification using iterative and non-iterative models. Additionally, the implementation of a ensemble learning is employed for optimally HSI object identification and classification.

2.1. Preprocessing

The system is loaded with the Indian Pines HSI dataset, which has 145×145 pixels and 220 spectral bands. The dataset also includes a ground truth label with 16 different classes, including various land cover types such as alfalfa, corn, grass-pasture, and stone-steel-towers. To better understand the spectral characteristics of the data, the system calculates the maximum and minimum wavelengths, which define the wavelength range of the spectral data. The data preprocessing step removes bands that correspond to water absorption regions, including bands 104 to 108, 150 to 163, and band 220. This careful cleaning of the data prepares it for subsequent analysis modules. These water absorption bands or regions in HSI refer to specific wavelengths of electromagnetic radiation where water molecules in the Earth's atmosphere absorb light. These absorption bands are characterized by reduced reflectance or transmittance of light due to the interaction between water molecules and incoming radiation. The reason behind removing water absorption bands is that it contains limited information about the surface materials and it can also interfere with the spectral signatures of the objects of interest in the scene.

2.2. Feature modelling

This section provides a detail discussion on the domain-based feature extraction process for HSI. This process will include selection of the optimal number of the spectral channels and enhancement of spatial information. The mechanism of feature modelling is carried out by optimal selection of spectral channels followed by adopting an adaptive gaussian method, and ensemble learning method. Elaboration of feature involved in proposed system is further discussed as following:

2.2.1. Selection of optimal spectral channels

Since, the HSI is of high dimension and often contains mixed pixel posing huge inter-class similarity and intra-class variability. Therefore, building an effective model often a requires to extract and

select the most informative spectral channels, eliminating redundant and irrelevant spectral data points. In this regard, the proposed system utilizes a PCA a widely used method for feature selection, which transforms the high-dimensional spectral data into a lower-dimensional space while preserving as much of the spatial information as possible. The selection of using PCA can be represented as in (5):

$$X \in \mathbb{R}^{\kappa \times M \times N} \leftarrow f1(x \in \mathbb{R}^{\lambda \times M \times N}, K) \quad (5)$$

In (5) shows process of optimal number of spectral bands $X \in \mathbb{R}^{\kappa \times (M \times N)}$ after applying PCA function $f1(\cdot)$ with an input argument of original preprocessed HSI data $x \in \mathbb{R}^{\lambda \times M \times N}$. The variable K denotes the number of optimal principal component which essentially equals to κ (number of spectral channels after PCA). Determining the suitable number of principal components is quite challenging task at initial as selection of K variable doesn't stem from dataset learning but is rather based on domain insights, specific requirements, and data interpretation. Selecting the K most informative principal components of X using PCA will reduce the impact of pixel mixing in the spectral domain, as the selected principal components will capture the most significant spectral variability in the data.

In Figure 2, the scree plot is shown for the PCA operation with K equals 30. This analysis further helps to decide more optimal number of principle component to choose. It can be analyzed that the first component explains the most variance, followed by the second component. Also, the amount of variance explained by each subsequent component decreases gradually. To determine how many principal components to retain, it can be seen for a point where the amount of variance explained begins to flatten out. In this case, it can observed that the first three principal components explain roughly two-thirds of the total variability in the standardized ratings, which is a substantial amount. Based on the graph trend, the study considers only 16 components that explain 95% of the total variance instead of the total 30 components.

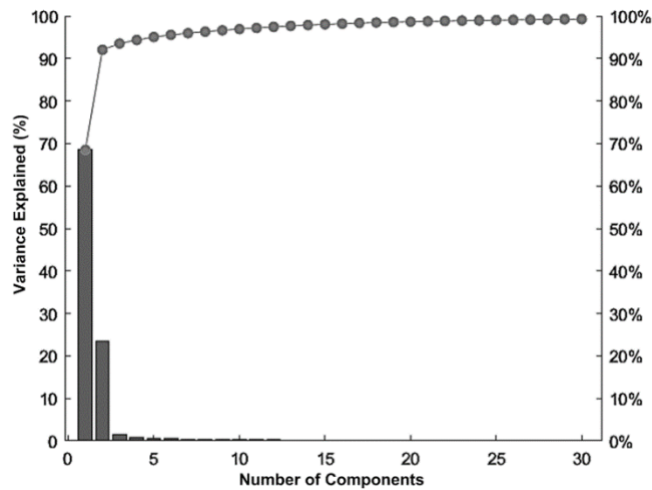


Figure 2. Analysis of scree plot for spectral feature selection

However, executing PCA over input HIS dataset, the data can exhibit certain characteristics that might introduce biases into subsequent analyses. The reason is that the PCA by its nature determines the principal components that capture the maximum variance in the data. However, this variance is influenced by the scale of the original features and such features with larger scales can dominate the variance, potentially leading to the misrepresentation of the importance of different features in the dataset. In this regard the study employed a data normalization scheme to avoid biasness in the dataset. The process of normalization adopted in this study aims to transform the hyperspectral data into a standard form where each feature (band) has a mean of 0 and a standard deviation of 1, numerically given in (6):

$$Z = \frac{x - \mu}{\sigma} \quad (6)$$

Where, Z is the standardized value, x refers to the input spectral band, μ is the average value, and σ denotes standard deviation of the all data-points in the spectral band, respectively. This normalization process ensures

that each band has a similar scale, as it removes the scale-related bias from the data with a mean of 0 and a standard deviation of 1, making it easier to compare and analyze the bands collectively.

2.2.2. Adaptive gaussian method

The research work presented in this paper proposes an adaptive Gaussian process as a spatial feature enhancement technique to improve the spatial resolution of HSI. The proposed method selectively smooths regions with low spatial variation while preserving edges and details in regions with high spatial variation. Unlike the conventional Gaussian filter, which uses a fixed kernel size, the proposed method introduces an adaptive kernel size based on the local image structure. The adaptive kernel size is more prominent in areas with high spatial variation and smaller in areas with low spatial variation. This ensures that the filter kernel size is better matched to the local structure of the image, resulting in improved image quality. The existing Gaussian filter is a linear filter often associated with ringing artifacts around the edges of the output image. In contrast, the proposed adaptive Gaussian method is a powerful non-linear filtering approach that adaptively adjusts the filter kernel's size depending on the image's local structure. This approach helps better to preserve edges and fine details in the image while reducing noise. Mathematically, for a given input HSI data $X(i, j)$ of size $M \times N$, the adaptive Gaussian process first determines the local spatial variation at each pixel location (i, j) by computing the variance of a local window around that pixel. This process can be numerically expressed as in (7):

$$V(i, j) = \text{var}(X(i + k, j + l)) \quad (7)$$

where (k, l) are the coordinates of the pixels in the local window centered at (i, j) . Next, a kernel size k is selected for each pixel location based on its local spatial variation $V(i, j)$. The kernel size is chosen such that smaller kernels are used in regions with high spatial variation, while larger kernels are used in regions with low spatial variation, given as (8):

$$k(i, j) = f(V(i, j), th) \quad (8)$$

where $f(\cdot)$ is an explicit function that maps the local variance $V(i, j)$ to a kernel size $k(i, j)$ using a threshold (th) on the local spatial variation to determine the size of the filter kernel, which ensures that larger kernel sizes are used in smooth regions of the image and smaller kernel sizes are used in regions with edges and fine details. Finally, a Gaussian operation is applied to each pixel using the selected kernel size $k(i, j)$ to smooth the image locally. This can be numerically expressed as (9):

$$X'(i, j) = G(i, j) \times X(i, j) \quad (9)$$

Where $X'(i, j)$ denotes output image with an enhanced spatial feature and $G(i, j)$ is a Gaussian kernel of size $k(i, j)$ centered at (i, j) . This phase of the proposed system helps avoid blurring important pixel signature in the image while reducing noise in the smoother regions. The novelty of the proposed adaptive Gaussian method is its ability to adapt to the local structure of the image, resulting in improved image quality, which can be particularly important in HSI, where the spectral and spatial information can vary widely within the same image. The further computing process is executed towards building training and testing dataset where training set is split with 30% of the dataset and remaining 70% of the dataset is kept for testing set. However, in general classification or predictive task majority of the dataset samples are kept for training the model. But in the context of HSI classification, where the number of features (spectral bands) is typically much larger than the number of samples (pixels), it is often necessary to choose a smaller training sample size to avoid overfitting and make the most efficient use of the available data. Basically, HSI data presents a scenario known as the curse of dimensionality, where there is a large number of features relative to the number of samples, which often lead to overfitting, where a model may perform well on the training data but fail to generalize to new, unseen data. Therefore, the study allocates a larger portion of the data for testing. It enables the model to be tested on a much broader and diverse set of samples, offering a more realistic assessment of its ability to generalize.

2.3. Ensemble learning

The proposed study has implemented two non-iterative learning schemes namely linear SVM and KNN and one iterative model namely ANN with dual hidden layer to perform classification. Based on the analysis of each model it has been identified that each model has different performance score subjected to different classes of the HSI dataset. The proposed study focuses on ensemble modelling to enhance the generalization capacity of the classification models. The rationale behind adopting ensemble modelling is

that different models may struggle with specific classes or scenarios due to the complex nature of hyperspectral data [25]. By employing ensemble learning, we can effectively address the variability in model performance, ensuring that the collective intelligence of all models is utilized to make classification decisions. Ensemble learning facilitates a more equitable contribution from each model, resulting in a comprehensive classification solution that accounts for varying strengths and weaknesses.

Figure 3 shows a flowchart of the proposed spectral-spatial classification system using ensemble learning for HSI classification. The system first loads the HSI data cube and removes the water absorption band. Then, it PCA with the initialization of 'K' principal components, leading to the acquisition of optimal spectral features prior to the data standardization process. Next, it enhances the spatial features of each spectral feature using adaptive Gaussian filtering. During this phase, the system sets up kernel 'k' and threshold Th for the adaptive Gaussian filtering procedure, enhancing the spatial resolution of each spectral feature. Finally, it splits the data into training and testing sets for the classification process. This stage trains SVM, KNN, and ANN models on the prepared dataset. The models are then used to generate prediction maps, which are analyzed to gain insights. Once the individual predictions have been made, ensemble modeling is used to combine the predictions of the different models using a maximum voting mechanism. This results in a final prediction map that integrates the spectral-spatial features and ensemble learning to ensure a comprehensive and nuanced classification of the HSI data.

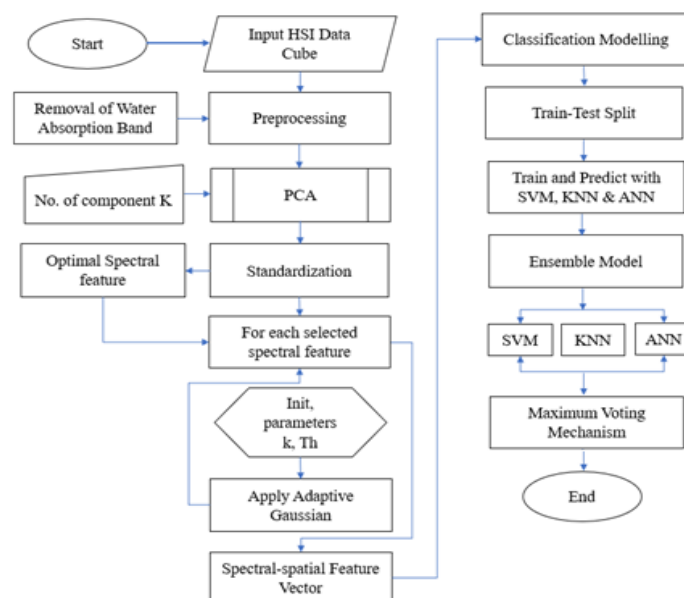


Figure 3. Flowchart of the proposed spectral-spatial and ensemble learning HSI classification

3. RESULT ANALYSIS

The development of the proposed system is carried out on the MATLAB tool, and performance analysis is done concerning different machine learning models. The proposed work considers three datasets, namely Indian Pine, Salinas, and Pavia, which are publicly available and have been extensively studied for the HSI classification problem [26]. The rationale behind choosing these HSI datasets for the evaluation of the proposed work is that these three HSI datasets offer a diverse range of spectral information and land cover classes and have been widely used and benchmarked in the remote sensing community. The performance analysis of the proposed system is assessed in terms of multiple matrices such as accuracy (measure of the overall correctness of the model), precision (represents the proportion of positive identifications that were actually correct), recall (represents the proportion of actual positives that were correctly identified), and F1-score (harmonic mean of precision and recall). In addition, the study also considers specificity (proportion of actual negatives that were correctly identified), error (ratio of the number of incorrect predictions to the total number of predictions), FPR (i.e., false positive rate which measures how many actual negatives were incorrectly identified as positive), MCC (matthews correlation coefficient is balanced measure which can be used even if the classes are of very different sizes), and Kappa score (measures the agreement between two raters for categorical objects) [27].

3.1. Analysis of the proposed system with Indian Pine dataset

The Indian Pine (IP) dataset was collected by the airborne visible/infrared imaging spectrometer (AVIRIS) sensor over an agricultural area in Indiana, USA. This dataset contains 145×145 pixels with 224 spectral bands covering the visible and near-infrared ranges [28]. The dataset represents 16 land cover classes, including corn, soybeans, and wheat, making it suitable for agricultural applications. Table 1 shows the performance of the implemented classification models on the IP dataset. The ensemble model outperforms all other models on all key metrics, achieving an accuracy of 99.51% and an error rate of 0.49%. This indicates that the ensemble model is highly accurate and robust in classifying HSI. The ANN model also performs well, achieving an accuracy of 97.42%.

Table 1. The outcome statistics of classification model for IP

| Metrics | SVM | KNN | ANN | Ensemble |
|-------------|--------|--------|--------|----------|
| Accuracy | 0.9611 | 0.9013 | 0.9742 | 0.9951 |
| Error | 0.0389 | 0.0987 | 0.0258 | 0.0049 |
| Recall | 0.9676 | 0.8684 | 0.9775 | 0.9944 |
| Specificity | 0.9971 | 0.993 | 0.9981 | 0.9997 |
| Precision | 0.979 | 0.8538 | 0.9789 | 0.9934 |
| FPR | 0.0029 | 0.007 | 0.0019 | 0.00034 |
| F1-score | 0.9729 | 0.8593 | 0.9779 | 0.9939 |
| MCC | 0.9702 | 0.8533 | 0.9762 | 0.9936 |
| Kappa | 0.6681 | 0.1578 | 0.7799 | 0.9584 |

The ensemble model's superiority is further evident in its high recall (99.44%), specificity (99.97%), and precision (99.34%). This means that the ensemble model is very good at identifying relevant instances and minimizing false identifications. The ensemble model also has a high F1-score and MCC, both exceeding 99%. This indicates that the ensemble model has a balanced performance and produces reliable classifications. The Kappa statistic of 0.9584 further validates the reliability of the ensemble model's classifications. Hence, ensemble model outperforms SVM, KNN and ANN, thereby demonstrates its effectiveness in generating high-quality classification maps for HSI.

Figure 4 shows the classification map of the IP HSI dataset, including the RGB representation, the ground truth map, the predicted map without feature modeling, and the final predicted map with the proposed feature modeling and ensemble learning. The ground truth map shows the actual pixel classifications, and it is used to compare the algorithm's predictions. A visual comparison of the predicted map and the ground truth map shows that they are very similar, which means that the algorithm is good at classifying pixels. The close alignment between the two maps shows that the algorithm is successful in accurately identifying the land cover features in the IP dataset.

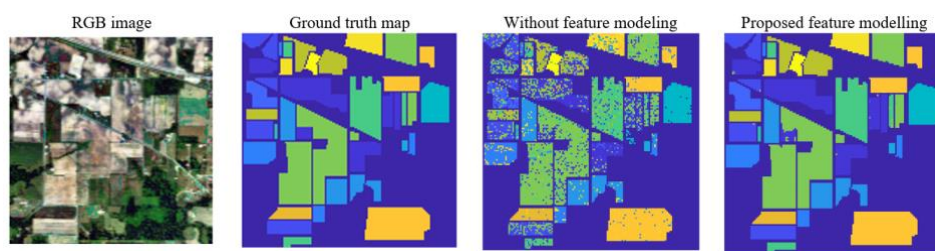


Figure 4. Predicted classification map for IP HSI data

3.2. Analysis of the proposed system with Salinas dataset

The AVIRIS sensor used to collect the data over an agricultural area in Salinas Valley, California, USA. This dataset contains 512×217 pixels with 224 spectral bands covering the visible and near-infrared ranges. The dataset represents 16 different land cover classes, including lettuce, broccoli, and bare soil, making it suitable for agricultural applications. Table 2 presents the performance of the implemented classification models on the Salinas dataset. The outcome analysis shows for this dataset also, the ensemble model outperformed all other models, achieving an accuracy of 99.99% and an error rate of 0.0001. This means that the ensemble model is extremely accurate and reliable at classifying pixels in the Salinas dataset.

The ensemble model also had a recall, precision, and F1-score of almost 1, which means that it is very good at identifying all relevant instances and has a balanced capability in precision and sensitivity. The ensemble model also had a perfect specificity and a very low FPR, which means that it is very good at avoiding false identifications. In addition, the it shows a higher MCC and Kappa score, which indicates that it produces high-quality binary classifications and has substantial agreement with the ground truth. On the other hand, the ANN model also performed well on the Salinas dataset, particularly in terms of specificity and MCC, while SVM and KNN models also yielded good results on the Salinas dataset, but the ensemble and ANN models were the best overall.

Table 2. The outcome statistics of classification model for Salinas

| Metrics | SVM | KNN | ANN | Ensemble |
|-------------|------------|------------|-------------|------------|
| Accuracy | 0.987 | 0.9932 | 0.9997 | 0.9999 |
| Error | 0.013 | 0.0068 | 0.00029031 | 0.0001 |
| Recall | 0.9947 | 0.9946 | 0.9994 | 0.9997 |
| Specificity | 0.999 | 0.9995 | 1 | 1 |
| Precision | 0.9949 | 0.9942 | 0.9996 | 0.9998 |
| FPR | 0.00098211 | 0.00048778 | 0.000019251 | 6.9298E-06 |
| F1_score | 0.9948 | 0.9944 | 0.9995 | 0.9998 |
| MCC | 0.9938 | 0.9939 | 0.9995 | 0.9998 |
| Kappa | 0.8892 | 0.9419 | 0.9975 | 0.9991 |

Figure 5 shows the classification map for the Salinas HSI dataset, including the RGB representation, the ground truth map, the predicted map without feature modeling, and the final predicted map with the proposed feature modeling and ensemble learning. The ground truth map shows the actual pixel classifications, and it is used to compare the algorithm's predictions. A visual comparison of the predicted maps and the ground truth map shows that they are very similar, especially the final predicted map, which closely matches the ground truth. This shows that the algorithm is good at classifying pixels and identifying the different land cover features within the Salinas dataset.

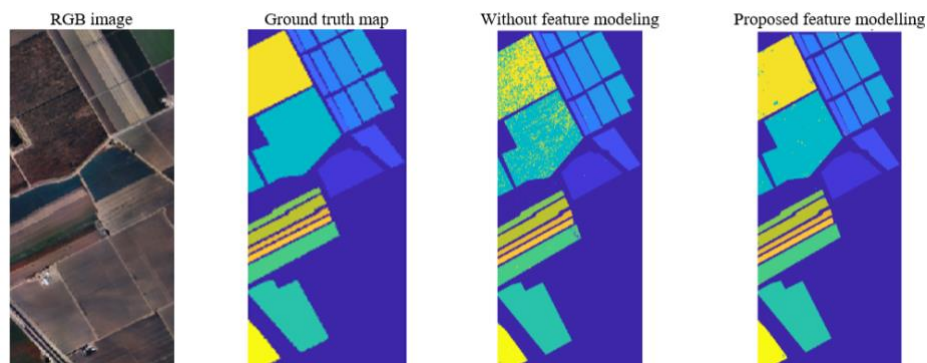


Figure 5. Predicted classification map for Salinas HSI data

3.3. Analysis of the proposed system with Pavia dataset

The reflective optics system imaging spectrometer (ROSIS) sensor acquired the Pavia dataset, Italy [29]. This dataset contains 610×340 pixels with 103 spectral bands covering the visible and near-infrared ranges. This dataset has nine land cover classes, including asphalt, meadows, and trees, making it suitable for urban land use applications. The outcome statistics for this HSI dataset is tabulated in Table 3.

The classification outcomes from the analysis in Table 3 proves that the leveraging potential of ensemble model provides a promising outcome for Pavia dataset, with an accuracy of 99.96% and an error rate of 0.00036736. This means that the ensemble model is extremely accurate and reliable at classifying data in the Pavia dataset. The ensemble model also had a recall, specificity, and precision of almost 1, which means that it is very good at identifying all relevant instances and avoiding false identifications. The ensemble model also had an F1-score and MCC of almost 1, i.e., 100 percent, which indicates that it has a harmonious balance between precision and recall and produces high-quality binary classifications. The Kappa value of 0.9981 for the ensemble model further underscores the substantial agreement between its predictions and the ground truth.

While the ANN and SVM models also performed well on the Pavia dataset, the ensemble model's results were significantly better which is also evident from the visual analysis provided in Figure 6. This demonstrates the unparalleled efficacy of the ensemble model and the promising potential of the proposed classification methodology for the Pavia dataset. The next sub-section presents the comparative analysis for the proposed with similar existing work.

Table 3. The outcome statistics of classification model for Pavia

| Metrics | SVM | KNN | ANN | Ensemble |
|---------------------|------------|--------|--------|------------|
| Accuracy | 0.9933 | 0.9788 | 0.9926 | 0.9996 |
| Error | 0.0067 | 0.0212 | 0.0074 | 0.00036736 |
| Recall | 0.988 | 0.9637 | 0.9864 | 0.9992 |
| Specificity | 0.9991 | 0.9973 | 0.999 | 1 |
| Precision | 0.9898 | 0.969 | 0.9912 | 0.9993 |
| False positive rate | 0.00093847 | 0.0027 | 0.001 | 0.00004 |
| F1_score | 0.9889 | 0.9663 | 0.9887 | 0.9993 |
| MCC | 0.988 | 0.9636 | 0.9878 | 0.9992 |
| Kappa | 0.9658 | 0.8925 | 0.9623 | 0.9981 |

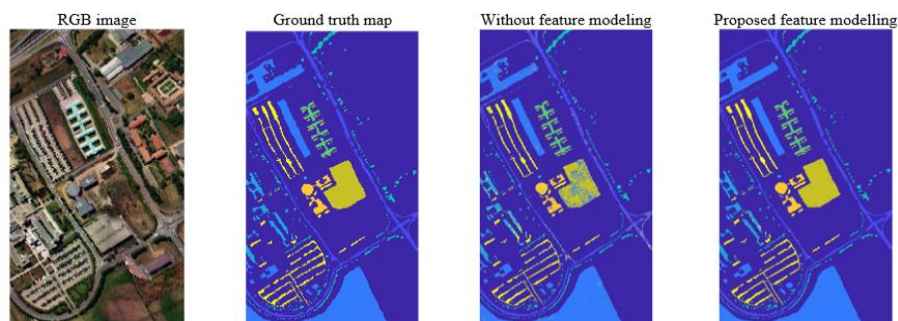


Figure 6. Classification map for Pavia HSI data obtained from ensemble learning

3.4. Comparative analysis

In order to justify the scope of the proposed work, the study conducts a comparative analysis considering the work carried out by Pathak *et al.* [24]. This work has exploited the potential of extended morphological profiles (EMP) for spectral-spatial pixel information encoding and SVM for classification. The comparative analysis depicted in Figure 7 demonstrates that the proposed model, outperforms the EMP-SVM model proposed in [24], concerning overall accuracy and Kappa score. The proposed model selects the best spectral features and enhances spatial features using an adaptive Gaussian filtering approach. In the Indian Pines dataset, the proposed model achieves an accuracy of 99.96% and a Kappa score of 99.81%, which is much better than the 91.09% accuracy and 89.78% Kappa score achieved by EMP-SVM. The proposed model also performs better than EMP-SVM on the Pavia and Salinas datasets. Overall, analysis shows that the proposed model is better at classifying HSI than the EMP-SVM model.

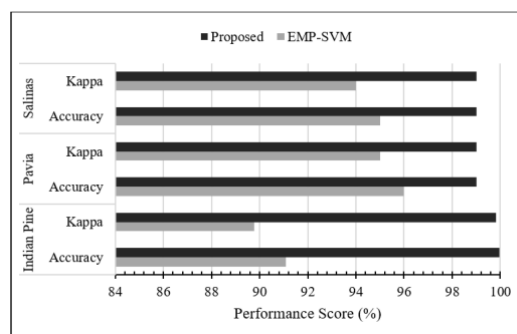


Figure 7. Comparative analysis concerning accuracy and kappa score

4. CONCLUSION

In this paper, the study propose a unique approach to enhance the accuracy and reliability of HSI classification by introducing a data-driven methodology focusing on optimal spectral-spatial feature enhancement and the potential of ensemble learning mechanisms. The prime aim was to develop an efficient and robust model that can produce high-quality classification maps of HSI data cubes without the need for complex learning models or extensive feature engineering. The implemented models are validated on three different HSI datasets, and it achieved near-perfect accuracy, specificity, precision, and Kappa scores on all three datasets. This outperforms existing approaches based on classical supervised classifiers. The effectiveness of the proposed approach is not only reflected in its superior statistical results, but also in its practical applicability, as visual comparisons between the predicted maps and the ground truth have shown very similar. This indicates that classification model with proposed spectral-spatial feature modeling accurately identifying land cover features in diverse datasets. In the future work, the proposed work will be extended towards exploring automated feature extraction using optimized deep learning models.




REFERENCES

- [1] B. Lu, P. D. Dao, J. Liu, Y. He, and J. Shang, "Recent advances of hyperspectral imaging technology and applications in agriculture," *Remote Sensing*, vol. 12, no. 16, 2020, doi: 10.3390/RS12162659.
- [2] G. Vivone, "Multispectral and hyperspectral image fusion in remote sensing: a survey," *Information Fusion*, vol. 89, pp. 405–417, 2023, doi: 10.1016/j.inffus.2022.08.032.
- [3] U. B. Gewali and S. T. Monteiro, "Multitask learning of vegetation biochemistry from hyperspectral data," in *Workshop on Hyperspectral Image and Signal Processing, Evolution in Remote Sensing*, IEEE, 2016, doi: 10.1109/WHISPERS.2016.8071800.
- [4] D. A. -Alimi, Z. Cai, M. A. A. A. -qaness, E. A. Alawamy, and A. Alalimi, "ETR: enhancing transformation reduction for reducing dimensionality and classification complexity in hyperspectral images," *Expert Systems with Applications*, vol. 213, 2023, doi: 10.1016/j.eswa.2022.118971.
- [5] W. Zhao and S. Du, "Spectral-spatial feature extraction for hyperspectral image classification: a dimension reduction and deep learning approach," *IEEE Transactions on Geoscience and Remote Sensing*, vol. 54, no. 8, pp. 4544–4554, 2016, doi: 10.1109/TGRS.2016.2543748.
- [6] S. S. Sawant and M. Prabukumar, "Semi-supervised techniques based hyper-spectral image classification: A survey," in *2017 Innovations in Power and Advanced Computing Technologies, i-PACT 2017*, IEEE, Apr. 2017, pp. 1–8, doi: 10.1109/IPACT.2017.8244999.
- [7] H. Nhaila, E. Sarhrouni, and A. Hammouch, "A survey on fundamental concepts and practical challenges of hyperspectral images," in *2014 2nd World Conference on Complex Systems, WCCS 2014*, IEEE, Nov. 2014, pp. 659–664, doi: 10.1109/ICoCS.2014.7060990.
- [8] M. Ahmad *et al.*, "Hyperspectral image classification - traditional to deep models: a survey for future prospects," *IEEE Journal of Selected Topics in Applied Earth Observations and Remote Sensing*, vol. 15, pp. 968–999, 2022, doi: 10.1109/JSTARS.2021.3133021.
- [9] R. Grewal, S. S. Kasana, and G. Kasana, "Machine learning and deep learning techniques for spectral spatial classification of hyperspectral images: a comprehensive survey," *Electronics*, vol. 12, no. 3, 2023, doi: 10.3390/electronics12030488.
- [10] M. Imani and H. Ghassemian, "An overview on spectral and spatial information fusion for hyperspectral image classification: current trends and challenges," *Information Fusion*, vol. 59, pp. 59–83, 2020, doi: 10.1016/j.inffus.2020.01.007.
- [11] R. Grewal, S. S. Kasana, and G. Kasana, "Hyperspectral image segmentation: a comprehensive survey," *Multimedia Tools and Applications*, vol. 82, no. 14, pp. 20819–20872, 2023, doi: 10.1007/s11042-022-13959-w.
- [12] W. Lv and X. Wang, "Overview of hyperspectral image classification," *Journal of Sensors*, vol. 2020, pp. 1–13, 2020, doi: 10.1155/2020/4817234.
- [13] Y. Su, X. Sun, L. Gao, J. Li, and B. Zhang, "Improved discrete swarm intelligence algorithms for endmember extraction from hyperspectral remote sensing images," *Journal of Applied Remote Sensing*, vol. 10, no. 4, Nov. 2016, doi: 10.1117/1.jrs.10.045018.
- [14] L. Zhang, Q. Zhang, B. Du, X. Huang, Y. Y. Tang, and D. Tao, "Simultaneous spectral-spatial feature selection and extraction for hyperspectral images," *IEEE Transactions on Cybernetics*, vol. 48, no. 1, pp. 16–28, 2018, doi: 10.1109/TCYB.2016.2605044.
- [15] H. Cen, R. Lu, Q. Zhu, and F. Mendoza, "Nondestructive detection of chilling injury in cucumber fruit using hyperspectral imaging with feature selection and supervised classification," *Postharvest Biology and Technology*, vol. 111, pp. 352–361, 2016, doi: 10.1016/j.postharvbio.2015.09.027.
- [16] A. Nakamura *et al.*, "Independent component analysis of hyperspectral data measured from overlapping latent fingerprints: Forensic potential of independent component images," *Forensic Science International*, vol. 343, 2023, doi: 10.1016/j.forsciint.2022.111549.
- [17] Y. Meng, R. Shang, L. Jiao, W. Zhang, Y. Yuan, and S. Yang, "Feature selection based dual-graph sparse non-negative matrix factorization for local discriminative clustering," *Neurocomputing*, vol. 290, pp. 87–99, 2018, doi: 10.1016/j.neucom.2018.02.044.
- [18] A. Falini *et al.*, "Saliency detection for hyperspectral images via sparse-non negative-matrix-factorization and novel distance measures," in *IEEE Conference on Evolving and Adaptive Intelligent Systems*, IEEE, 2020, pp. 1–8, doi: 10.1109/EAIS48028.2020.9122749.
- [19] L. Demarchi, A. Kania, W. Ciekowski, H. Piórkowski, Z. O. -Piasko, and J. Chormański, "Recursive feature elimination and random forest classification of natura 2000 grasslands in lowland river valleys of poland based on airborne hyperspectral and LiDAR data fusion," *Remote Sensing*, vol. 12, no. 11, 2020, doi: 10.3390/rs12111842.
- [20] J. Feng, L. Jiao, F. Liu, T. Sun, and X. Zhang, "Mutual-information-based semi-supervised hyperspectral band selection with high discrimination, high information, and low redundancy," *IEEE Transactions on Geoscience and Remote Sensing*, vol. 53, no. 5, pp. 2956–2969, 2015, doi: 10.1109/TGRS.2014.2367022.
- [21] B. Du, L. Zhang, D. Tao, and D. Zhang, "Unsupervised transfer learning for target detection from hyperspectral images," *Neurocomputing*, vol. 120, pp. 72–82, Nov. 2013, doi: 10.1016/j.neucom.2012.08.056.
- [22] X. Wang, K. Tan, Q. Du, Y. Chen, and P. Du, "CVA2E: a conditional variational autoencoder with an adversarial training process for hyperspectral imagery classification," *IEEE Transactions on Geoscience and Remote Sensing*, vol. 58, no. 8, pp. 5676–5692, 2020, doi: 10.1109/TGRS.2020.2968304.




- [23] U. Sakthivel, A. P. Jyothi, N. Susila, and T. Sheela, "Conspectus of K-means clustering algorithm," in *Applied Learning Algorithms for Intelligent IoT*, 2021, pp. 193–213, doi: 10.1201/9781003119838-9.
- [24] D. K. Pathak, S. K. Kalita, and D. K. Bhattacharya, "Hyperspectral image classification using support vector machine: a spectral spatial feature based approach," *Evolutionary Intelligence*, vol. 15, no. 3, pp. 1809–1823, 2022, doi: 10.1007/s12065-021-00591-0.
- [25] I. D. Mienye and Y. Sun, "A survey of ensemble learning: concepts, algorithms, applications, and prospects," *IEEE Access*, vol. 10, pp. 99129–99149, 2022, doi: 10.1109/ACCESS.2022.3207287.
- [26] L. Sun, J. Zhang, J. Li, Y. Wang, and D. Zeng, "SDFC dataset: a large-scale benchmark dataset for hyperspectral image classification," *Optical and Quantum Electronics*, vol. 55, no. 2, 2023, doi: 10.1007/s11082-022-04399-9.
- [27] I. M. D. Diego, A. R. Redondo, R. R. Fernández, J. Navarro, and J. M. Moguerza, "General performance score for classification problems," *Applied Intelligence*, vol. 52, no. 10, pp. 12049–12063, 2022, doi: 10.1007/s10489-021-03041-7.
- [28] T. T. Pham *et al.*, "Airborne object detection using hyperspectral imaging: deep learning review," in *Lecture Notes in Computer Science (including subseries Lecture Notes in Artificial Intelligence and Lecture Notes in Bioinformatics)*, Springer International Publishing, 2019, pp. 306–321, doi: 10.1007/978-3-030-24289-3_23.
- [29] R. Buschner, R. Doerffer, and H. V. D. Piepen, "Imaging spectrometer ROSIS," in *Laser/Optoelektronik in der Technik / Laser/Optoelectronics in Engineering*, Berlin, Heidelberg: Springer, 1990, pp. 368–373, doi: 10.1007/978-3-642-48372-1_77.

BIOGRAPHIES OF AUTHORS



Bhavatarini Nagendra    holds B.E. in Information Science and Engineering and M.Tech. in Computer Science and Engineering. She is a research scholar at M. S. Ramaiah University of Applied Sciences. She is currently working as assistant professor at the School of Computer Science and Engineering, REVA University, Bangalore, Karnataka. She has eight years of teaching experience and is a member of International Association of Engineers (IAENG) and Institute of Electrical and Electronics Engineers (IEEE). Her special fields of interest include machine learning, deep learning, hyperspectral imaging, and mobile Ad hoc networks. She can be contacted at email: bhavatarini.n@reva.edu.in.



Jyothi Aracot Prashant    completed her Ph.D. in 2020 from VTU, India. She is currently working as assistant professor in Department of Computer Science and Engineering, Faculty of Engineering and Technology, M. S. Ramaiah University of Applied Sciences, Bengaluru. She has 17 years of experience in teaching and has published many papers in journals indexed in SCI/SCIE, WoS, and Scopus. She presented papers in several national and international conferences. Her research interest is in the field of wireless sensor network, MANET, IoT, AI, ML, and deep learning. She is a member of LMISTE, LMIAENG, AMIETE, IFERP, LMINSO, and IEEE. She is a reviewer for Springer, Wiley, IEEE, Elsevier, IGI, oriental journals, and international conference papers from Taiwan, Prague, Czech Republic, and Japan. She has authored book chapter in Springer, Wiley, IET, CRC Press Talyor, and Francis group. She has received best women researcher award and several research excellence awards. She has an Indian patent published, an international patent granted, and an Indian patent filed in her name. She can be contacted at email: jyothi.cs.et@msruas.ac.in or jyothiaracotprashant@gmail.com.